The Impact of Melting Ice Sheets on Future Global Climate

Dimitri Defrance, Thibault Catry, Amélie Rajaud, Nadine Dessay, Benjamin Sultan

EarthArXiv coversheet for:

The Impact of Melting Ice Sheets on Future Global Climate

Dimitri Defrance, Thibault Catry, Amélie Rajaud, Nadine Dessay and Benjamin Sultan

Dimitri Defrance

*corresponding author :

 E-mail: dimitri.defrance@inra.fr

 RG : https://www.researchgate.net/profile/Dimitri_Defrance

SYSTEM, Univ Montpellier, INRA, Montpellier SupAgro, CIRAD, CIHEAM, 2 Place Pierre Viala, Bâtiment 27, 34060 Montpellier, France

ESPACE-DEV, UMR 228 IRD/UM/UR/UG/UA, Institut de Recherche pour le Développement (IRD), Maison de la Télédétection, 500 Rue Jean François Breton, 34090 Montpellier

Thibault Catry, Nadine Dessay, Benjamin Sultan

ESPACE-DEV, UMR 228 IRD/UM/UR/UG/UA, Institut de Recherche pour le Développement (IRD), Maison de la Télédétection, 500 Rue Jean François Breton, 34090 Montpellier

Amélie Rajaud

IPSL/Sorbonne Université, 4 Place Jussieu, 75005 Paris, France

The Impact of Melting Ice Sheets on Future Global Climate

Dimitri Defrance[a,b,*], Thibault Catry[b], Amélie Rajaud[c], Nadine Dessay[b] and Benjamin Sultan[b]

[a]SYSTEM, Univ Montpellier, INRA, Montpellier SupAgro, CIRAD, CIHEAM, 2 Place Pierre Viala, Bâtiment 27, 34060 Montpellier, France

[b]ESPACE-DEV, UMR 228 IRD/UM/UR/UG/UA, Institut de Recherche pour le Développement (IRD), Maison de la Télédétection, 500 Rue Jean François Breton, 34090 Montpellier

[c]IPSL/Sorbonne Université, 4 Place Jussieu, 75005 Paris, France

* corresponding author : dimitri.defrance@inra.fr

Abstract

Climate change studies in the last decades have been based on Global Climate Models (GCM), and the distribution of climatic regions over time extracted from these models can be represented using the Köppen climatic classification. The Köppen approach predicts the distribution of biomes worldwide on the basis of monthly precipitation and average temperature. This study aims to use the Köppen classification to evaluate the impact of the Greenland and Antarctic ice sheets melting on GCM simulation results at the regional and global scale. To assess the impact of accelerated ice-sheet melting, our approach is based on numerical simulations from the IPSL-CM5A-LR GCM with the introduction of freshwater near the ice sheets superimposed on the RCP8.5 scenario, leading to a global warming of +5°C. Static mapping of distribution changes in Köppen climatic regions under various scenarios (historical run from observations, RCP 8.5, and various cases of polar sheets melting) and comparisons between them reveal that major changes occur at the global scale for the period 2041-2060. A first level of analysis revealed that, when the input of freshwater originates from Greenland or Antarctica, the inter-tropical belt undergoes greater change than under the RCP8.5 scenario. A second level of analysis showed that changes in precipitation have major impacts on the southern hemisphere, with more drastic changes if the freshwater came from the Greenland ice sheet than if it came from Antarctica or from the combination of both. Changes in temperature, however, strongly impact the northern hemisphere, and are significantly affected by the melting of the Greenland ice sheet. This study highlights the importance of considering ice sheets melting in the modelling of future global climate.

Keywords: climate modelling, ice sheet melting, climate change, Köppen classification

1- Introduction

Climate change and its impacts on society and ecosystems have been investigated for the last decades using Global Climate Models (GCM), which provide projections of future climate under various emission scenarios (Manabe and Stouffer, 1980; McGuffie et al., 1999; Delworth et al., 2006; Moss et al., 2010; Semenov and Stratonovitch, 2010). The Representative Concentration Pathways (RCP) produce a range of CO_2 emission pathways corresponding to the radiative forcing in 2100 (see Taylor et al., 2012) within the frame of the Coupled Model Intercomparison Project (CMIP-5, Meehl et al., 2000).

Driven by climate change, polar ice sheet melting is accelerating, resulting in a massive input of freshwater into the oceans (Peterson et al., 2006; Rignot et al., 2011), which is not accounted for in the CMIP5 projections (Church et al., 2013). However, a recent review showed that under the 2°C warming scenarios, the ice sheet melting is irreversible and accelerates during the 21st century (Pattyn et al. 2018). Various studies showed that this process has already affected past and present climatic dynamics (Dahl-Jensen et al., 1998; Hansen et al., 2016; Swingedouw et al., 2008 and 2015). During the last glacial maximum, an acceleration of the ice sheet melting, the so called Heinrich event, occurred and drastically changed the global climate (Alvarez-Solas and Ramstein, 2011). For example, paleoclimatic surveys and numerical modeling experiments reported a weakening of the monsoons in Africa (Mulitza et al., 2008) and India (Marzin et al., 2013), an increase of El Niño– Southern Oscillation(ENSO) amplitude (Luan et al., 2015), more rainfall in Australia (Denniston et al., 2013), an intensification of rainfall in Amazonia (Lewis et al., 2010) and cooler temperatures in Europe (Guiot et al., 1993) and North America (Grimm et al., 1993). Not accounting for these mechanisms in future projections may thus lead to overlooking serious consequences of climate change. Here we use a simulation approach developed by Defrance et al. (2017) to test the effects of freshwater input from ice sheets melting on the climatic changes simulated for RCP 8.5.

Beyond a simple analysis of the GCMs' outputs, an integrative approach based on bioclimatic classification can be used to give an ecological understanding of the combined changes in climate variables and to assess how the location and extent of present climatic regions will evolve over time (*e.g.* Trewartha and Horn, 1980; Kalvova et al., 2003; Feng et al., 2014; Belda et al., 2015). The Köppen climate classification is the most widely used classification method (Rubel and Kottek, 2010 ; Rajaud and de Noblet-Ducoudré, 2017). Based on expert knowledge of the climatic conditions that cause generic biomes, it defines a set of climatic regions separated by empirical thresholds of temperatures and rainfall. These are used to predict the distribution of biomes worldwide on the basis of monthly cumulative precipitation, monthly mean air temperature, and the relationship between climate and vegetation (Köppen, 1900, 1923, 1931 and 1936; Geiger, 1954 ; Fraedrich et al., 2001; Rubbel and Kottek, 2010). Its ability to reproduce observed geographical biome patterns has been validated by Rohli et al., 2015. This classification has been used to study climatic shifts in many regions (Fraedrich et al., 2001; Rubbel and Kottek, 2010; Rajaud and de Noblet-Ducoudré, 2017). Following a similar approach, Thornthwaite's climate classification includes refined delimitation criteria; although more recent, its higher level of complexity makes it more difficult to apply and to interpret, and it is much less used than the Köppen classification (Feddema, 2005). An alternative approach to making sense of climatic changes is statistical clustering over a larger ensemble of climate variables (Metzger et al., 2013). However, the ecological significance of the statistical partition thus produced can only be validated through comparison to a reference, which often is the Köppen classification. We followed the most common approach for this paper and used the Köppen classification.

This study aims to compare the impacts of freshwater inputs from the Greenland and/or Antarctic ice sheets melting by the end of the 21st century under the RCP 8.5 scenario , which leads to an approximately 5 °C increase in global temperature, on:

- the simulated global evolution of temperature and precipitation,
- the distribution and shifts of climatic regions using Köppen classifications at global scale
- the regional trends of climatic evolution in South America, Africa and Australia complementary to results obtained for West Africa using the same approach by Defrance et al., 2017.

2- Methodology

2.1- Climate model and experimental design

The experimental design used in this study is based on a methodological approach developed by Defrance et al. (2017), which is summarized in figure 1.

All the experiments presented in this study have been carried out with the coupled atmosphere-ocean IPSL-CM5A-LR model (Dufresne et al., 2013) which has been used for the CMIP5 exercise (Taylor et al., 2012). The model contains biogeochemistry models (troposphere to the deep ocean) and physical models (atmosphere, land surface, ocean and sea-ice). Natural and anthropogenic perturbations are taken into account through CO_2 emissions, other greenhouse gases, changes in land use, solar irradiance and volcanic aerosols. The atmospheric component (LMDZ) has a spatial resolution of 3.75° X 1.875° in longitude and latitude respectively with 39 vertical levels. The oceanic component (NEMO) uses an irregular grid with a nominal resolution of 2°, and a finer latitudinal resolution of 0.5° in the equatorial ocean, and 31 vertical levels.

Using the IPSL-CM5A-LR GCM run under the RCP8.5 radiative forcing scenario from 2006 to 2100, we added a continuous freshwater flux (FWF) of 0.11, 0.22, 0.34 and 0.68 Sv, (where 1 Sv=$10^6 m^3$ s^{-1}) from 2020 to 2070, leading to 0.5, 1, 1.5 and 3 m of cumulative sea level rise . As a consequence, six scenarios (in addition to the baseline) are considered, in which the freshwater flux may come either from Greenland only (GrIS scenarios) or from West Antarctica only (WAIS scenarios) or from an equal contribution of both ice sheets (GrWAIS scenarios):

- RCP 8.5 (baseline scenario), no freshwater input
- RCP 8.5 + 0.5, 1 , 1.5 and 3 m of freshwater input from Greenland melting only
- RCP 8.5 + 3m of freshwater input from Antarctica melting only
- RCP 8.5 + 3m of freshwater input from combined Antarctica and Greenland meltings

For Antarctica only and the combined melting, we only included the 3 m sea level rise in the study since the model is not responsive to lower freshwater inputs. The locations of freshwater inputs have been chosen to produce a rapid response of the model. Freshwater has therefore been released in locations with deep water formations in the North Atlantic for GrIS and GrWAIS scenarios (45°N-65°N, 45°W-5°E) and in the western part of the Southern Ocean for WAIS and GrWAIS scenarios. The choice of high FWF values (0.11 to 0.68 Sv) is justified by the fact that current climate models are believed to be not sensitive enough to freshwater input (Hansen et al., 2016; Swingedouw et al., 2013). Accounting for large amounts allows us to better evaluate their potential global impact.
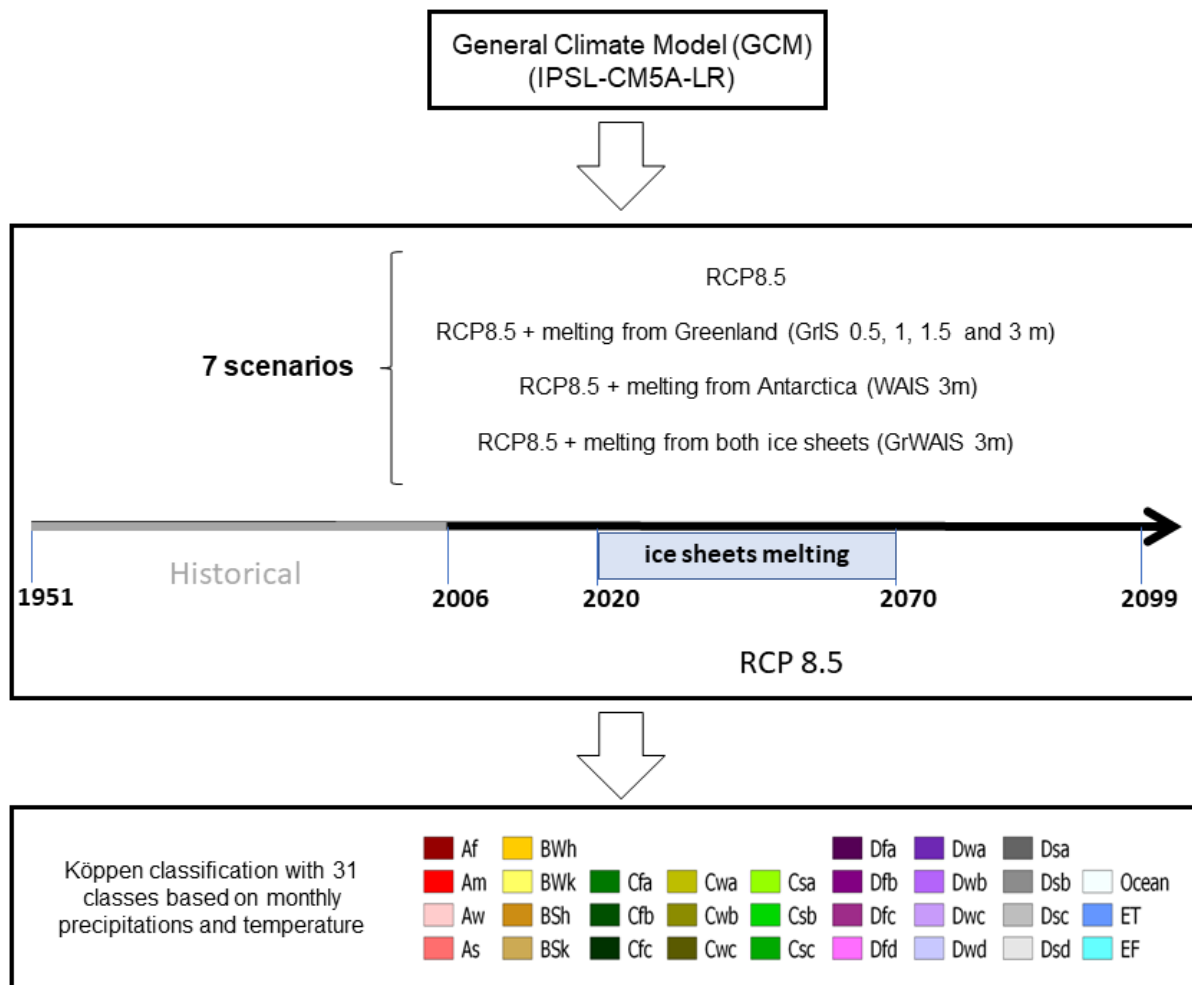
Figure 1: Methodological workflow used in this study combining numerical simulations from the IPSL-CM5A-LR GCM and the RCP8.5 scenario with Köppen classifications to produce evolution scenarios of climatic areas over the period 1951-2100.

2.2- Bias-correction of climate simulations

GCMs' bias for the current climate can hamper the application of climate classification based on absolute rainfall and/or temperature thresholds. For instance, precipitation IPSL-CM5A-LR has a temperature bias of -1.4°C on average (Dufresne et al., 2013.) and some biases for precipitation such as a lower than observed monsoonal rainfall (Famien *et* al., 2018) in West Africa, or too frequent rainfall in the Andes mountains (see Dufresne et al., 2013 for more details). In West Africa, Famien et al. (2018) weaken the bias on the daily data by using an univariate quantile-quantile method called the Cumulative Distribution Function transfert (CDFt) method (Michelangeli et al., 2009, Vrac et al., 2012). By computing various climatic indices such as seasonal rainfall, dry spells and onset of the rains, Famien et al. (2018) demonstrated that this technique strongly reduces the errors in the CMIP5 models compared to observed data (EWEMBI, http://dataservices.gfz-potsdam.de/pik/showshort.php?id=escidoc:1809891, Frieler et al., 2017). Although univariate, this method maintains the link between temperature and precipitation established in the model. Here, the same techniques are used to compute daily temperature and precipitation across the entire world under the RCP8.5, GrIS, WAIS and GrWAIS scenarios over the period 1951-2100 with a resolution of 0.5°X0.5°. Finally, daily rainfall (temperature) is accumulated (averaged) on a monthly time step to define the Köppen classification.

In order to assess the reliability of the bias correction, we produced a kappa index between the observed data (EWEMBI) and the bias-corrected historical simulation. This index is a statistic which measures qualitatively the correlation (agreement) between two items, such as the Köppen classification results in our study (kappa reaches 1 when the correlation is maximized). The accuracy assessment using the kappa calculation is based on the selection of a statistically representative sampling of the reference dataset pixels (here EWEMBI Run, fig. 4a, is assumed to be accurate) and to determine if the produced classification (here Historical Run, fig. 4b) assigned to that pixel matches the true classification of that pixel on the reference.

2.3- Köppen classification

Based on bias-corrected monthly precipitation and temperature, the Köppen classification is defined by five main climatic groups, named from A (equatorial climates) to E (polar climates). Groups B, C and D respectively stand for "arid", "warm temperate" and "snow" climates. Each group is further divided into sub-groups, using empirical temperature and precipitation thresholds. In total, we used 31 classes based on different formulations that can be found in Kottek et al. (2006, see supplementary material 1 for a table containing group and subgroup labels and associated conditions). To limit the impact of year-to-year variability in temperature and precipitation, we computed climate averages over 20 years between 2041 and 2060 for the above listed scenarios, in agreement with previous studies by Rajaud et al. (2017) and Feng et al. (2014). In addition, we computed a reference situation for the period 1986-2005 obtained using the IPSL-CM5A-LR model and the EWEMBI data, used for bias correction. This reference period allows us to assess our correction using the 31 Köppen classes. We described group and sub-group changes. Group changes refer to shifts from one main Köppen group to another (A, B, C, D, and E, see supplementary material for more details) while sub-group changes refer to shifts within a single group (for instance, in group A, shifts from sub-group As to subgroup Am). In the Köppen labels, the second letter refers to the precipitation regime while the third letter refers to temperature. More details about the methodology used in this paper can be found on the companion data paper (co-submitted).

3- Results

After studying the global change in temperature and precipitation under various scenarios (fig. 2 and 3), we investigate the global evolution of climatic region distribution. We first focuse on changes under the RCP8.5 scenario (fig. 5), then on group changes (fig. 6 and 7) and finally on sub-group changes (fig. 8 and 9), under the melting scenarios described earlier.

3.1- Global changes in temperature and precipitation

Figure 2a presents the mean annual temperature over the period 1986-2005 (referred to here as the historical run). Figures 2b, c and d show the variations in global temperature with respect to the historical run for the period 2041-2060 under the RCP 8.5, the GrIS 3m and the WAIS 3m scenarios respectively. Other scenarios are introduced in the supplementary materials (SI2&3). For the RCP 8.5 case, maximum variations in temperature are observed in the northern hemisphere at high latitudes (Greenland and Scandinavia) reaching 5 to 10 °C locally. Lower variations are located in equatorial regions (around 1.5 °C). These high values of temperature change are related to the fact that the IPSL model simulates the stronger changes in future temperatures for the CMIP5 (Dufresne et al., 2013). For the GrIS 3m scenario, the melting of the Greenland ice sheet induces a cooling of 1°C in Greenland and the British Islands. The northern hemisphere is affected by a reduced warming (2 to 4°C). Warming in Equatorial regions is stronger, reaching 2 to 4°C. For the WAIS 3m, a similar warming to RCP 8.5 is observed in the northern hemisphere, but at a larger scale. In equatorial

regions, RCP 8.5 and WAIS 3m are in general agreement, with minor local differences in South America and Africa.
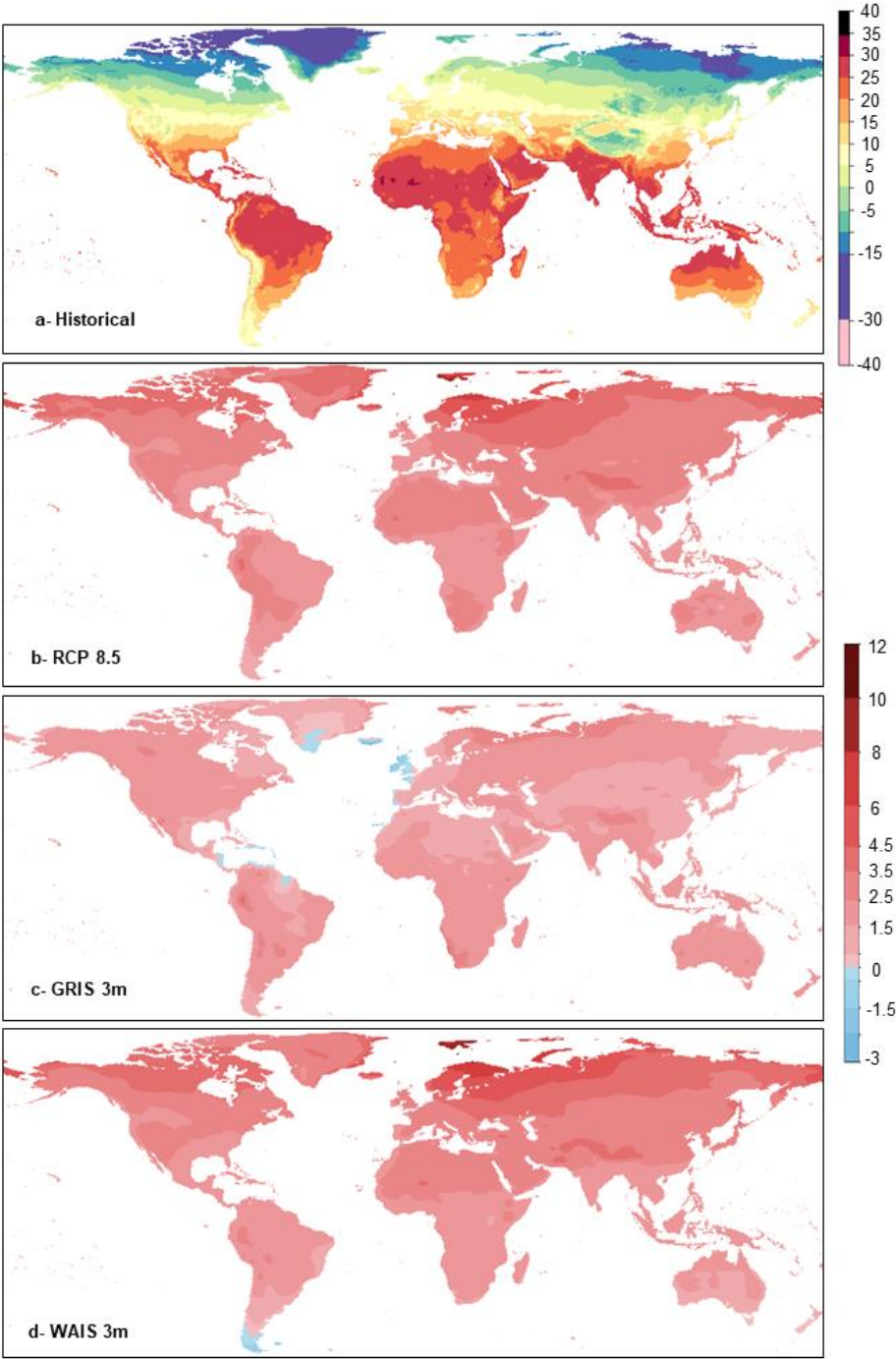

Figure 2: Mean annual temperature for the historical IPSL-CM5A-LR run for (a) the period 1986-2005 and global changes in temperature (in °C) for the period 2041-2060 under scenarios (b) RCP 8.5, (c) GrIS 3m and (d) WAIS 3m.

Figure 3a presents the mean annual precipitation over the period 1986-2005 (referred to here as the historical run). Figures 3b, c and d show the variations of global precipitation with respect to the historical run for the period 2041-2060 under the RCP 8.5, the GrIS 3m and the WAIS 3m scenarios respectively. Other scenarios are introduced in supplementary material. Modelling results for the RCP 8.5 scenario, using IPSL-CM5A-LR, show minor changes in precipitation in the northern hemisphere (with an increase less than 250 mm/year). Central America and western south America (pacific side) get drier, with decreases in precipitation reaching 750 mm/year). North Africa, West Africa, South Africa and Australia are affected by a decrease of precipitation less than 250 mm/year. Equatorial regions experience wetter conditions with an increase ranging between 1000 and 1500 mm/year (see Brazil for example, fig. 3c). Under the GrIS 3m scenario, precipitation weakens in Europe and northern America (up to 250 mm/year). For central and southern America, the changes are similar as in RCP 8.5 but the intensities of the phenomena are stronger: a decrease in precipitation reaching 1500 mm/year and an increase of 3000 mm/year respectively. Western and Central Africa are drier (-750 mm/year), while South Africa and Australia are wetter (+1000 mm/year). For the WAIS 3m, similar results as the RCP 8.5 are simulated at high latitudes. Variations are inverted in comparison with RCP 8.5 in central (more rainy conditions) and southern America (less rainy conditions). More precipitation occurs in Central and western Africa, while less precipitation occurs in Australia.
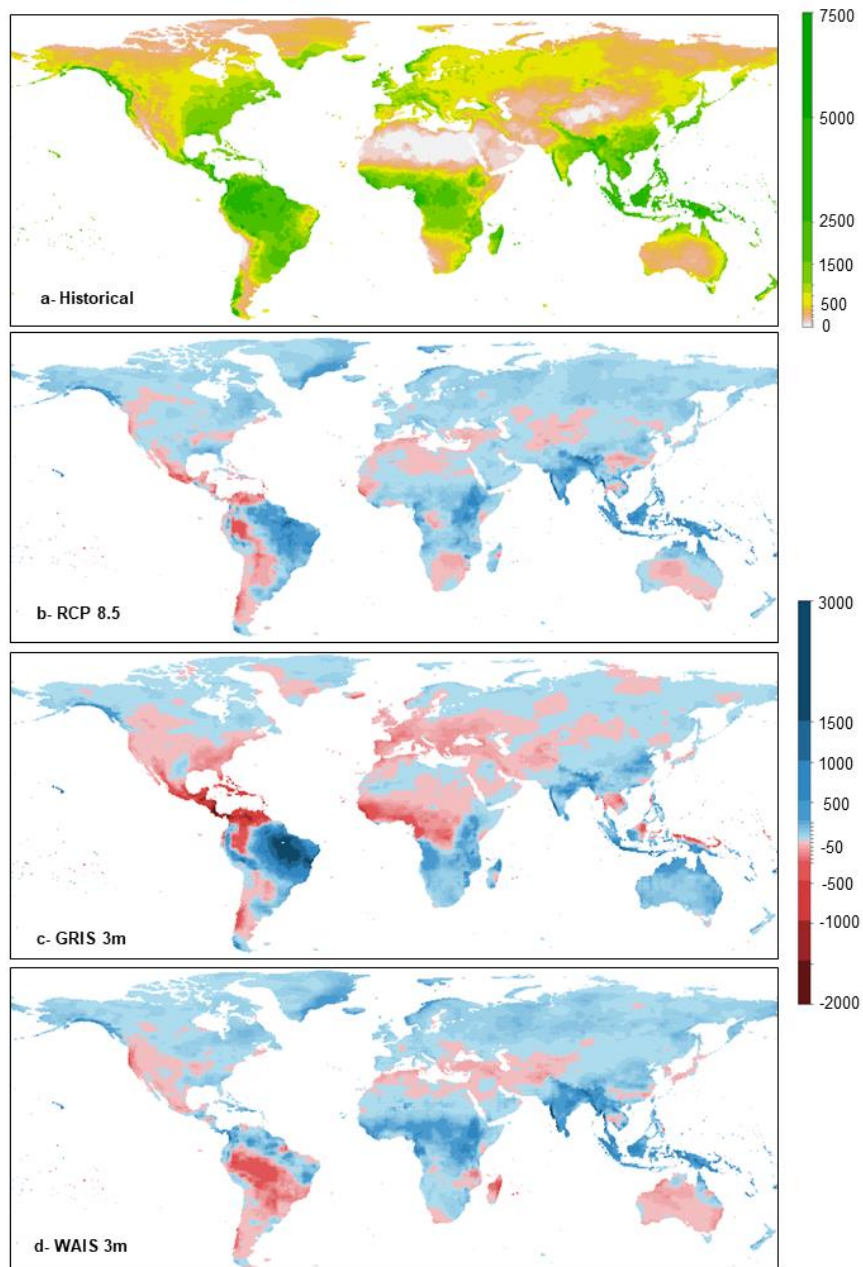
Figure 3: Mean annual precipitation for (a) the historical IPSL-CM5A-LR run for the period 1986-2005 and global changes in precipitation (in mm) for the period 2041-2060 under the (b) RCP 8.5, (c) GrIS 3m and (d) WAIS 3m scenarios.

3.2- Distribution of climatic regions at global scale

The classifications obtained using the EWEMBI dataset for the period 1986-2005 (fig. 4a) from observation data is compared to a similar results obtained using the IPSL-CM5A-LR model bias-corrected with the methods developed by Famien et al. (2018, fig. 4b). Both classifications are in good agreement with a correlation kappa index of 0.96. Modelling results and observations are consistent, thus validating our GCM historical simulations.
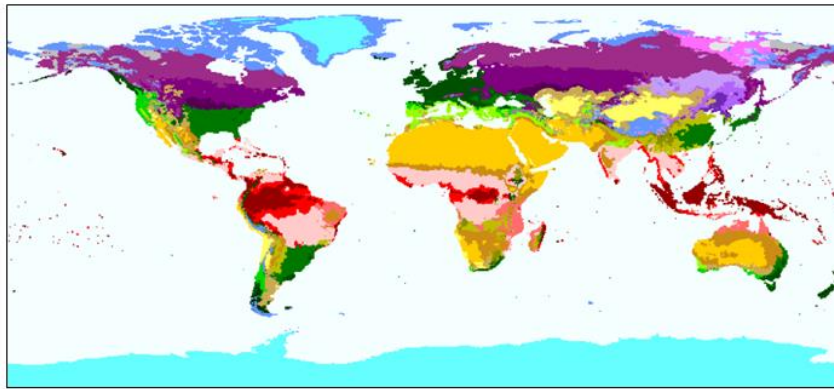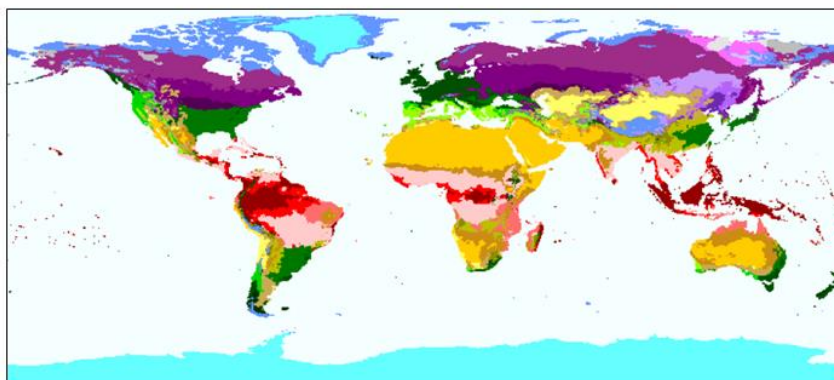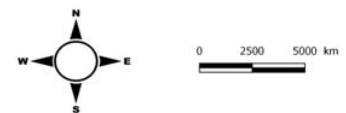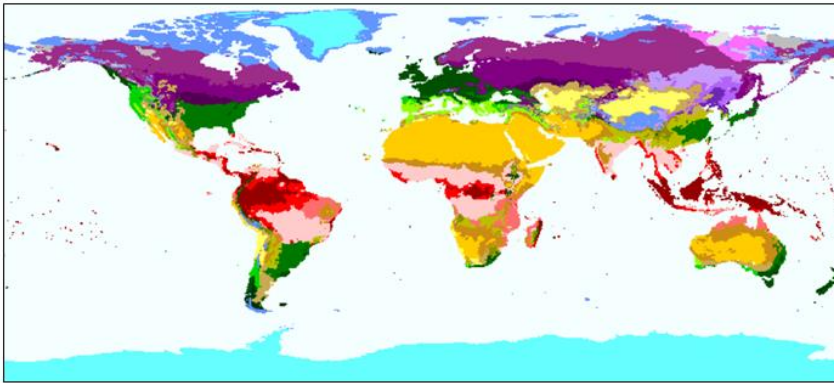
Figure 4: Köppen classification results at a global scale. (a) EWEMBI classification result from observation data (historical run 1986-2005), (b) results obtained using the IPSL-CM5A-LR bias-corrected model (historical run 1986-2005).

3.2.1- Evolution under RCP8.5 scenario.

The different Köppen classes are computed for the period 2041-2060 with the precipitation and temperature time series simulated by the IPSL-CM5-LR model under the RCP8.5 scenario. Our results exhibit similar trends compared to other studies obtained by other GCMs (e.g. Beck et al., 2018 and Feng et al., 2014), confirming the robustness of our approach. In Northern America, a shift from Dfc (Snow climate, fully humid Cool summer) to Dfa (Snow climate, fully humid Hot summer and cold winter) is simulated when temperatures increase. In Western Europe, changes in group C is highlighted with the sub-group Csa (Warm temperate climate with dry and hot summer) replacing sub-group Csb (Warm temperate climate with dry and warm summer) in Southern Europe. In Eastern Europe and Russia, group C (Warm temperate climates) gains ground on group D (Snow climates) and as in Northern America, the sub-group Dfc is reduced due to the increase in temperature. The increase of subgroup Bw (Desert climate) is simulated for Africa (around the Sahara and Kalahari deserts), Australia and Mexico. In monsoon zones (in South America, Africa and South East Asia), we have a shift towards group A (Equatorial climates), related to changes in precipitation (increase or decrease).
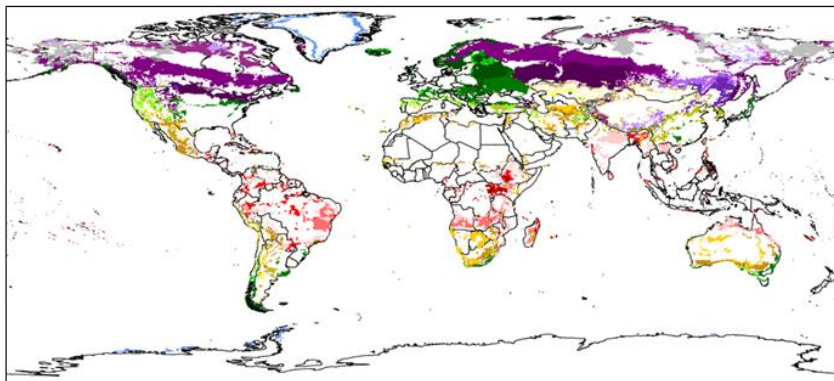
Figure 5: Köppen classification results at a global scale. (a) historical run for 1986-2005 and (b) RCP8.5 run for 2041-2060, obtained using the IPSL-CM5A-LR bias-corrected model.

3.2.1 Inter-Group changes

Figures 6 and 7 show the evolution of the groups of the Köppen classification by comparing the melting scenarios in 2041-2060 with the RCP8.5 scenario for the same period. For all scenarios, group E is primarily modified only by changes related to group D (Figure 6). For scenarios with Greenland ice melt, we observe an increase in Group E area (up to +1.74 million km² for the GrIS3m scenario), located in Northern America and Iceland.

Group A (equatorial climate) is affected by a loss of surface for the scenarios associated with a melting of the Greenland ice sheet (GrIS and GrWAIS) with a maximum loss of 2.03 million km² in the GrIS3m case. In this case, this decrease can be explained by the 2.2 million km² that become group B (Arid climates) in South America and on the southern edge of the Sahara in Africa (Figure 7b) mitigated by gains in other regions such as Australia in the place of the group B (Figure 7b). These group changes are linked to the variations in precipitation (cf Table SI1). Group B has a surface gain in the GrIS and GrWAIS scenarios with a maximum gain of 0.62 million km², unlike the WAIS3m which suffers a loss of 0.42 million km². This evolution is related to group A, but also to group C (Warm temperate climates). Indeed, in the case GrIS3m, 1.13 million km² become part of group C (Figure 6a), mainly in Australia (Figure 7b). The area of group C decreases when the Greenland ice sheet melts (maximum for GrWAIS 3m with -1.47 million km², Figure 6c) and increases by 0.61 million km² for WAIS3m (Figure 6b). In this scenario, the increase is related to a transition from Group D (Snow climates) to Group C in Europe and Northern America (Figure 7b) related to temperature changes. Finally Group D has a gain in area related to the melting of Greenland at the expense of group C and a loss in the case WAIS3m. The changes are mainly located in Europe and Northern America (Figure 7). The other Greenland scenarios show similarities with GrIS 3m and are presented in SI4.
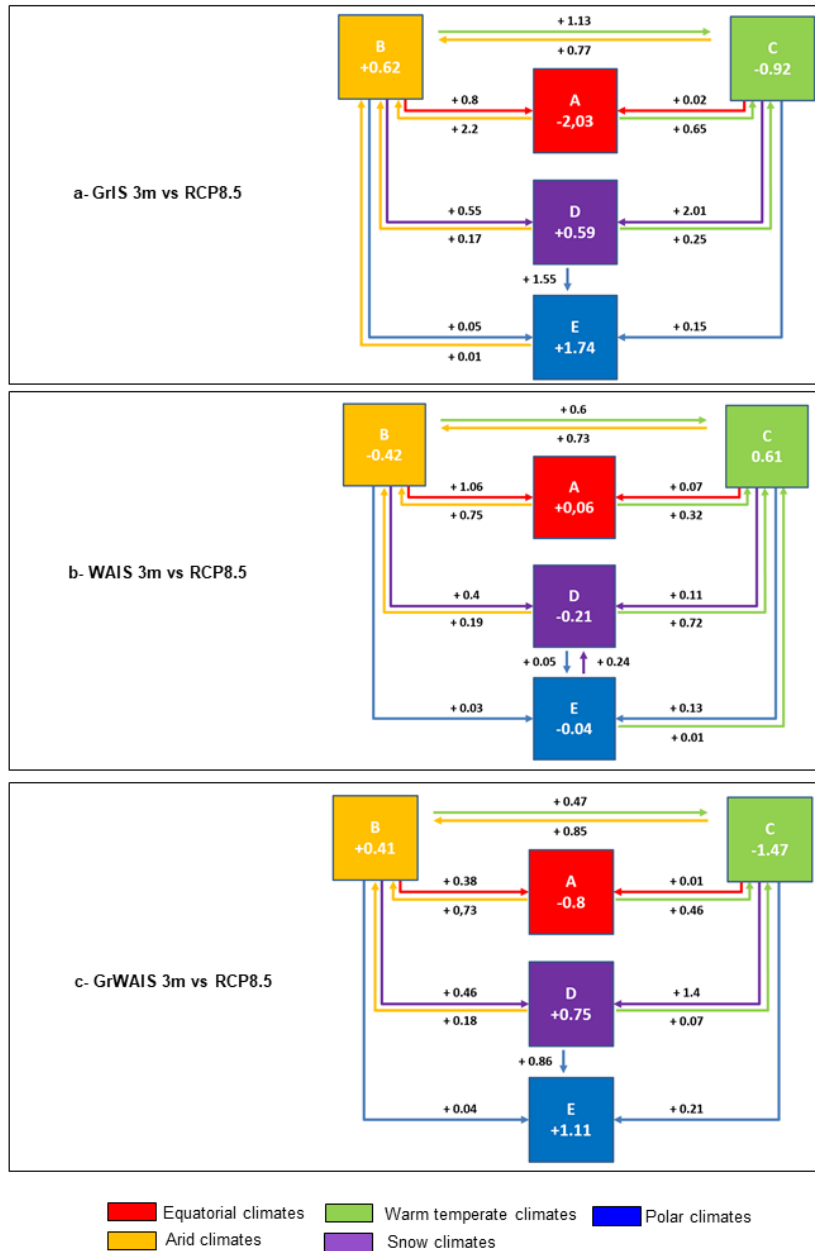
Figure 6: Quantification of surface group changes in million km² under (a) the GrIS 3m, (b) the WAIS 3m and (c) the GrWAIS 3m scenarios for the period 2041-2060, with respect to the RCP8.5 baseline.
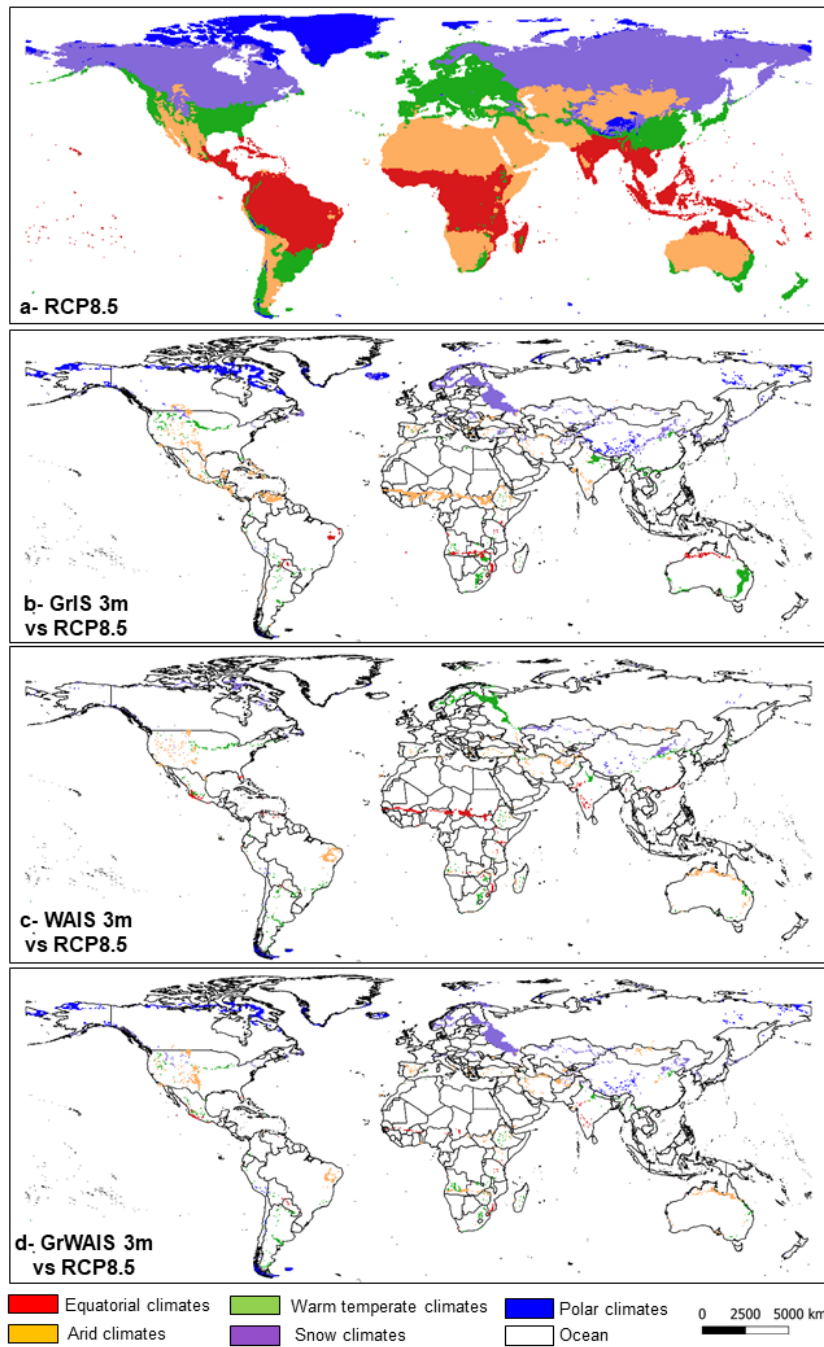
Figure 7: Köppen classification results showing group changes (A, B, C, D and E) between (a) the RCP 8.5 and (b) the GrIS 3m, (c) the WAIS 3m and (d) the GrWAIS 3m for the period 2041-2060. Colors represent the appearance of new classes, areas in white being not affected by inter-class changes. Other scenarios (0.5, 1 and 1.5 m water input) are in the supplementary materials.

3.2.2- Sub-group changes

Impact of precipitation changes on sub-group distribution

Precipitation changes showe no major impact on the Köppen classification of the northern hemisphere, whatever the considered scenario, except at the highest latitudes, where over northern America, northern Europe and Russia, Dfb (wet continental climate) replaces Dfc and Dfd (subarctic climate). The shifts are more pronounced for GrIS 3m and GrWAIS 3m (fig. 8) and other GrIS scenarios (0.5, 1 and 1m in SI5).

The southern hemisphere, on the contrary, is strongly impacted by precipitation changes with diverse responses and intensities for the 3 scenarios. Most important changes with respect to the baseline RCP8.5 scenario (fig. 8a), are seen under the GrIS 3m scenario (fig. 8b) (and GrIS 1.5 m SI5), in which South America, Africa and Australia exhibit large scale and/or intense sub-group shifts. In south America, shift occur throughout the entire upper continent, As (Equatorial savannah with dry summer) and Aw (Equatorial savannah with dry winter) shifts to Am (Equatorial monsoon) and Am shifts to Af (Equatorial rainforest, fully humid). Thus, rainforests and monsoon forests expanded globally, at the expense of savannas. In Africa, in sub-Saharan regions, deserts (Bw) expands southward at the expense of steppes (Bs), and the boundary of the Sahara shifts towards lower latitudes. For south-African regions, the opposite shift is simulated. In central Africa, Equatorial rainforest (Af) shifts towards Equatorial monsoon (Am). In Australia, desert (Bw) is replaced by steppe (Bs). Under the WAIS 3m (fig. 8c), the major change in Africa was the retreat of the southern boundary of the Sahara where the desert (Bw) becomes steppe (Bs). In South America and Australia, shifts are more local and less intense. Finally, similar shifts, with lower intensities are observed under the GrWAIS 3m and WAIS 3m scenarios (fig. 8d).
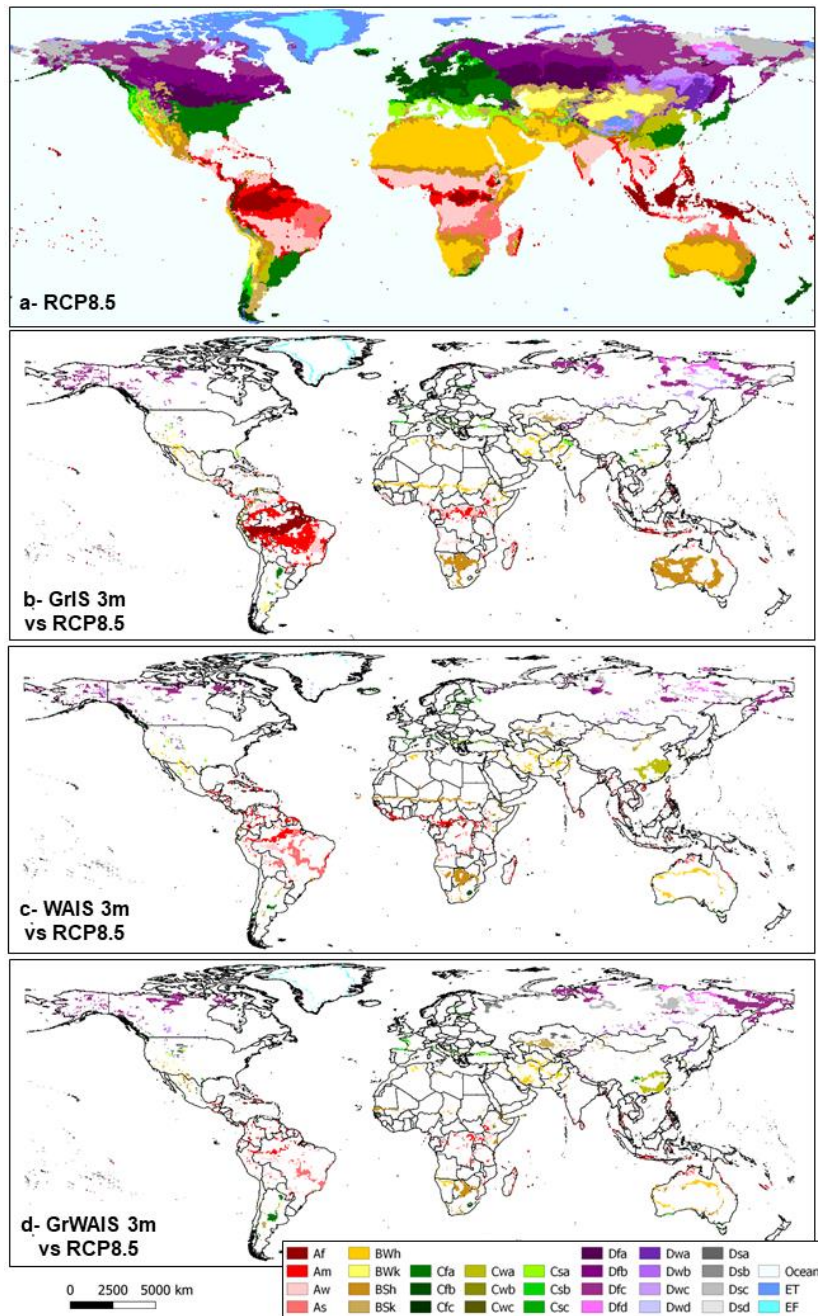
Figure 8: Köppen classification results showing precipitation-related sub-group changes (3rd letter on the Köppen nomenclature) between (a) the RCP8.5 and (b) the GrIS 3m, (c) the WAIS 3m and (d) the GrWAIS 3m scenarios for the period 2041-2060. Colors represent sub-group shifts, areas in white being unaffected by sub-group changes. Other scenarios (0.5, 1 and 1.5 m water input) are in the supplementary materials.

Impact of temperature changes on sub-group distribution

Changes in temperature show no impact on the sub-groups' distribution in the southern hemisphere (fig. 9) under any scenario compared to the baseline RCP8.5 (fig. 9a). The main impacts occur on the northern hemisphere. Under the GrIS 3m (fig. 9b) and the GrWAIS 3m (fig. 9d) scenarios, shifts are similar in nature. In northern America, northern Europe and Russia, Dfa (warm continental climate) is

replaced by Dfb (semi-boreal climate) and Dfb shifts towards Dfc (subartic or boreal climate). Shifts are more intense under GrIS 3m than under GrWAIS 3m. The other GrIS scenarios (SI6) show similar changes in the North hemisphere. Under the WAIS 3m scenario, central Europe is the most impacted region, with Cfb (oceanic climate) and Cfc (subpolar oceanic climate) shifting towards Cfa (humid subtropical climate) throughout the entire region.

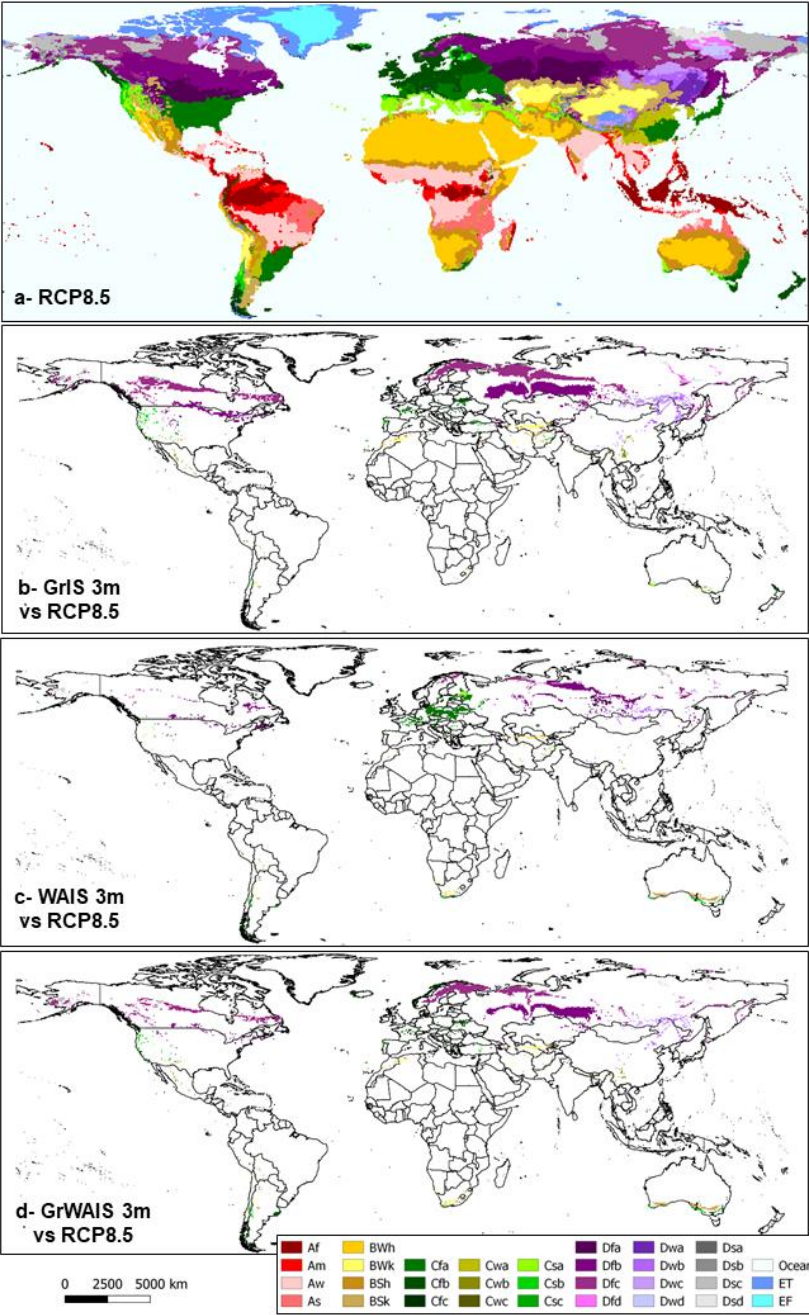*Figure 9: Köppen classification results showing temperature-related sub-group changes (3rd letter on the Köppen nomenclature) between (a) the RCP8.5 and (b) the GrIS 3m, (c) the WAIS 3m and (d) the GrWAIS 3m scenarios for the period 2041-2060. Colors represent sub-group shifts, areas in white being unaffected by sub-group changes. Other scenarios (0.5, 1 and 1.5 m water input) are in the supplementary materiasl.*

4- Discussion

This study used the Köppen classification to assess the consequences of an acceleration in ice-sheet melting by the end of the 21st century using the IPSL-CM5A-LR model. To simulate the melting, an introduction of freshwater in the North Atlantic or around West-Antarctica was superimposed on the RCP8.5 scenario. Based on the monthly average temperature and cumulative precipitation we obtained a reasonable fit of the Köppen classification between observations (EWEMBI) and historical simulation.

Biases corrections

Figure 4 shows that our bias correction is efficient. Defrance et al. (2017) and Famien et al. (2018) showed severe misrepresentations of precipitation distribution, especially in Africa, if this correction was not performed. In this case, it would not be possible to carry out a precise description of intra-class shifts as we did in Figure 6, for instance, in the Sahara region. From a global perspective, a detailed description of inter and intra class shifts requires overcoming the limitation of modelling results, i.e. integrating a thorough correction of biases. The bias correction method we implemented is univariate and therefore each variable has been corrected independently from the other, despite the existing link between temperature and precipitation. Studies by Feng et al. (2014) and Beck et al. (2018) used similar univariate methods to investigate Köppen-based climate changes. Recently, some authors proposed approaches to overcome the bias due to temperature and precipitation correlation based on multivariate bias correction methods (Maraun et al., 2016; Cannon, 2016; Cannon, 2018). However these approaches are very recessive, and used in smaller areas. An application to the world would require more important resources of computation and additional analyzes that we could not do.

Temperature and precipitation changes vs. climate shifts

Our results confirmed the observations obtained by Feng et al. (2014) and Mahlstein et al. (2013) who have shown that RCP8.5 sub-group changes are mainly related to changes in temperature in the northern hemisphere and to changes in precipitation in the southern hemisphere.

Focusing on sub-group changes, regardless of the scenario, shifts from Bw to Bs and from As to Am/Af are related to variations in precipitation thresholds (fig. 8). Figure 8 shows that shifts observed in the southern hemisphere are the consequence of changes in precipitation, for instance in Australia and South America, where sub-group shifts can be explained by the general increase in precipitation, with values greater than 1000 mm under the GrIS3m scenario (fig. 8b and 3). As climates are already hot, temperature variations have no major influence on the distribution of climate groups. In Australia, the increase in precipitation is accompanied by a drop in temperatures, compared to the RCP8.5, on the order of 1°C (Fig. 2c). Mahlstein et al. (2013) indicated that temperature and precipitation threshold used in the Köppen classifications are defined as minima and maxima. However, since the initial conditions in some regions are above or below these thresholds, some variations might not induce climate group shifts. These results are also the consequences of the way the Köppen classification model is built, in which for groups A and B, temperatures are high (over 18°C) with lower variations under the tropics.

The case of the acceleration of the Greenland ice melt shows, for the northern Hemisphere, major changes in the Köppen classification due to temperature (fig. 9a). The limitation of the increase in temperature to + 2.5 ° C maximum (fig. 2c), lower by about 1 to 1.5 °C compared to RCP8.5 (fig. 2b), for the period 2041-2060 justifies the reduction of the impact on the classification for the 21st

century. In the southern hemisphere, drastic changes in the Köppen classification are observed in several regions such as West Africa, Oceania and South America. By analyzing the evolution of temperatures (fig. 2) and precipitation patterns (fig. 3), the latter are strongly disturbed with a drying up of West Africa, which explains the passage from group A to group B (difference based on precipitation), and corresponds to an extension of the Sahara to the south. The case of Brazil strongly highlights the importance of precipitation over temperature in the case of climate shift. Indeed, under GRiS 3m, major sub-group changes in the A group occur in Brazil, as evidenced by fig. 8b. Figures 3 and 8 show a strong correlation between precipitation variations (reaching + 3000 mm/year) and sub-group shifts. Although the variation in temperature is stronger under GriS 3m than under other scenarios, the impact on climate groups distribution over Brazil remains secondary.

Antarctica vs. Greenland contribution to climate shift

Figures 7, 8 and 9 support that, for the WAIS 3m scenario, the effects are less marked than for the GrIS 3m scenario, due to the isolation of the continent by the Antarctic circumpolar stream (Nowlin and Klinck, 1986; Whitworth, 1988; Martinson, 2012). The similarities with RCP8.5 for the northern hemisphere are directly related to temperature and precipitation changes similar to those of RCP8.5. For the southern hemisphere, temperatures are lower by about 1°C compared to RCP8.5. For precipitation, the results accentuate the trend of RCP8.5 with very contrasting situations: a decrease of rainfall in South America up to 500 mm (Fig. 3d), a generalized increase over Africa, especially across West Africa with increases up to 1000 mm, and in Australia, which is drier, drops up to 500 mm in the North-West and South-East. These observations are opposed to those made with the GrIS 3m scenario. Our changes in temperature and precipitation corroborate a recent study by Bronselaer et al. (2018) which, with a freshwater scenario from West-Antarctica superimposed on the RCP8.5 scenario with another climate model, has similar temperature and precipitation changes: very little difference in temperature compared to RCP8.5 and a shift of the Intertropical Convergence Zone (ITCZ) to the North causing drier areas in Oceania and South America and a wetter Sahel region.

The addition of uncertainty related to the melting of the caps

Our study shows that a higher volume of freshwater is necessary for Antarctica to have consequences on the climate. Current observations show that the contribution from Greenland is more important than West Antarctica by a factor 2 (Pattyn et al. 2018). For projections, the future is very uncertain, and the contribution of Antarctica could be extremely important after 2050 (Kopp et al., 2017) and taking over the leading role from Greenland.

The disturbance caused by the melting of ice sheets, however, can increase the uncertainty of the IPCC projections. For example, in the intertropical zone subject to monsoons, North America Monsoon System (NAMS), North Africa (NAF), South America Monsoon System (SAMS) and South Africa (SAF) are associated with high uncertainty about future precipitation that could increase or decrease depending on the model (Christensen et al., 2013). For example,the addition of Greenland or Antarctic melt will add uncertainty to NAF that could respectively increase or decrease depending on the freshwater source. To a lesser extent, SAMS could be strongly or weakly reinforced depending on the origin of the water supply in the ocean. On the contrary, for Southern Asia (SAS) and East Asian Summer (EAS), and the Australian-Maritime Continent (AUSMC) Asian monsoons, the CMIP5 models are more in agreement in predicting an increase in precipitation (Christensen et al., 2013) that does not seem to be strongly influenced by the melting of Greenland or Antarctic ice sheets. For the northern hemisphere where, the Köppen class change is mainly temperature-related, the different CMIP5 models are consistent with an increase of the temperature (Collins et al., 2013). Therefore, the impact of Greenland ice melt will only be able to limit the RCP8.5 scenario change and therefore the Köppen class changes.

High uncertainty is associated with monsoons in South America and Africa as there is not always consistency between CMIP5 model projections and conflicting simulated effects of freshwater input into the ocean. On the contrary, for the Northern Hemisphere and the monsoons of Asia and Northern Australia, the ice caps have a smaller role and the CMIP5 models are more concordant.

Comparison with paleoclimate

All these changes related to different melting scenarios have been observed in the past and the mechanisms that induced them can be extrapolated to the future. During the Last Glacial Maximum (LGA), there were episodes of rapid upheaval, known as Heinrich events. During these events, rapid changes in the northern hemisphere's ice sheet with a decrease in the Gulf Stream, which involved a redistribution of heat from the equator to the poles (Swingedouw et al., 2009; Alvarez-Solas and Ramstein, 2011,). The consequences were a decrease in the temperature of the North Atlantic and an increase of it in the South Atlantic causing climate change on the whole planet. The northern hemisphere cooled quickly during these episodes in connection with the decrease of the Gulf Stream as indicated for example by the studies of Grimm et al. (1993) and Kerschner et al. (2008). For the tropical zone, it is the variation in precipitation which is highlighted during the Heinrich events. For the drying up of West Africa, the decrease in temperature in the North, towards the Sahara, combined with a warmer South Atlantic, modified the monsoon cycles which penetrated less far North than currently causing mega-drought episodes (Mulitza et al., 2008, Defrance et al., 2017). In Oceania, ITCZ's shift southward favored precipitation over northern Australia (Denniston et al., 2013). Finally in South America we observed an increase in precipitation, e.g. in the Altiplano with lake Tauca (Martin et al., 2018) or in the North of Brazil (Dupont et al., 2010), in connection with a shift to the south of the ITCZ and a redistribution of the prevailing winds facilitating the penetration of moisture across the continent.

As for the paleoclimatic consequences associated with freshwater flux from Antarctica, to the best of our knowledge, there are no studies linking records of freshwater input associated with abrupt climatic changes. However, sensitivity tests with various levels of freshwater introduction in the South Atlantic have been made and show reverse phenomena (in terms of temperature and precipitation) compared to what happens when the water comes from Greenland (e.g. Stouffer et al. 2007; Swingedouw et al., 2008).

The consequences related to the acceleration of the melting of the caps seem to be consistent with robust mechanisms given by paleographic records and different multi-model studies on the evolution of the temperatures and the precipitation during Heinrich events (e.g. Stouffer et al., 2006; Swingedouw et al., 2009). The main limitation of our study is to rely only a single model, which does not allow us to take into account the inter-model variability highlighted by different studies like Feng et al. (2014). Simulations of freshwater introduction should be performed with other climate models to better account for the variability of adding freshwater. Nevertheless, Swingedouw et al. (2009) and Stouffer et al. (2006) showed that the effects on the southern hemisphere with heat redistribution were robust which corroborates the trends we have observed. In addition, the amount of water introduced may seem important, however, several studies have shown that our current models may not be sufficiently sensitive to the addition of freshwater from ice sheets (see methodology and Sgubin et al. 2017).

5- Conclusion

Heinrich events during the last glacial maximum warn of the climatic consequences of accelerated ice sheet melt. Since the last IPCC report (AR5), several studies have shown that the ice sheets could melt faster than previously predicted and might induce global climatic change beyond sea level rise. Using the IPSL-CM5A-LR climate model, we have demonstrated the impact of accelerated ice sheet melting on 21st century climate change. Several studies have shown, using the Köppen classification, that there will be an expansion of arid zones in the 21st century (eg. Rajaud et al., 2017). However, none took into account the acceleration of the ice sheet melt (Peterson et al., 2006; Rignot et al., 2011). Our study showed that freshwater, introduced into the North Atlantic or the Antarctic Ocean, exacerbated or mitigated some of the changes already induced by RCP8.5. Regionally, an acceleration of the melting of the Greenland ice sheet will further modify the Sahel region with an expansion of the desert climate towards the south. South America will experience a higher rainfall with a monsoon or tropical climate and Australia's desert biomes will shift towards a steppe. Impacts on the northern hemisphere will be limited and will counteract the changes induced by the RCP8.5 scenario. On the other hand, the destabilization of West Antarctica will have a more limited effect, as the Southern Ocean is isolated from other oceans by the Antarctic circumpolar current. Some regions will undergo significant changes, such as the southern Sahara shifting towards steppes. With this study, we showed the importance of taking ice sheet melt into account in climate projections, as it is associated with higher model uncertainty in some regions, such as West Africa.

Those changes, together with projected demographic changes, will increase the portion of the population exposed to changing precipitation patterns, especially in the southern hemisphere, with consequences on humans and societies which are not currently accounted for. However, analyzing climate evolution using the Köppen approach does not consider inter-annual variability or extreme events and only provides mean trends. Moreover, despite the analogies with past climates, our results are based on only one climatic model with idealized simulations. These will have to be confirmed by the use of other climate models because there are a variety of responses among models, including differences in the predictedtime frame of climate change.

References

Alvarez-Solas, J. and Ramstein, G. (2011). On the triggering mechanism of Heinrich events, Proc. Natl. Acad. Sci., 108(50), E1359–E1360, doi:10.1073/pnas.1116575108.

Beck, H. E., Zimmermann, N. E., McVicar, T. R., Vergopolan, N., Berg, A., & Wood, E. F. (2018). Present and future Köppen-Geiger climate classification maps at 1-km resolution. Scientific data, 5, 180214.

Belda, M., Holtanová, E., Halenka, T., Kalvová, J., & Hlávka, Z. (2015). Evaluation of CMIP5 present climate simulations using the Köppen-Trewartha climate classification. Climate Research, 64(3), 201-212.

Bronselaer, B., Winton, M., Griffies, S. M., Hurlin, W. J., Rodgers, K. B., Sergienko, O. V., Stouffer, R. J., Russell, J. L.(2018). Change in future climate due to Antarctic meltwater. Nature, doi:10.1038/s41586-018-0712-z.

Cannon, A. J. (2016). Multivariate bias correction of climate model output: Matching marginal distributions and intervariable dependence structure. Journal of Climate, 29(19), 7045-7064.

Cannon, A. J. (2018). Multivariate quantile mapping bias correction: an N-dimensional probability density function transform for climate model simulations of multiple variables. Climate dynamics, 50(1-2), 31-49.

Church, J. A., Clark, P. U., Cazenave, A., Gregory, J. M., Jevrejeva, S., Levermann, A., Merrifield, M. A., Milne, G. A., Nerem, R. S., Nunn, P. D., Payne, A. J., Pfeffer, W. T., Stammer, D. and Unnikrishnan, A. S.: Sea Level Change, in Climate Change 2013: The Physical Science Basis. Contribution of Working Group I to the Fifth Assessment Report of the Intergovernmental Panel on Climate Change [Stocker, T.F., D. Qin, G.-K. Plattner, M. Tignor, S.K. Allen, J. Boschung, A. Nauels, Y. Xia, pp. 1137–1216., 2013.

Collins, M., Knutti, R., Arblaster, J., Dufresne, J. L., Fichefet, T., Friedlingstein, P., … & Shongwe, M. (2013). Long-term climate change: projections, commitments and irreversibility, in Climate Change 2013: The Physical Science Basis. Contribution of Working Group I to the Fifth Assessment Report of the Intergovernmental Panel on Climate Change [Stocker, T.F., D. Qin, G.-K. Plattner, M. Tignor, S.K. Allen, J. Boschung, A. Nauels, Y. Xia, pp. 1137–1216., 2013.

Christensen, J. H., Kanikicharla, K. K., Marshall, G., & Turner, J. (2013). Climate phenomena and their relevance for future regional climate change, in Climate Change 2013: The Physical Science Basis. Contribution of Working Group I to the Fifth Assessment Report of the Intergovernmental Panel on Climate Change [Stocker, T.F., D. Qin, G.-K. Plattner, M. Tignor, S.K. Allen, J. Boschung, A. Nauels, Y. Xia, pp. 1137–1216., 2013.

Dahl-Jensen, D., Mosegaard, K., Gundestrup, N., Clow, G. D., Johnsen, S. J., Hansen, A. W., & Balling, N. (1998). Past temperatures directly from the Greenland ice sheet. Science, 282(5387), 268-271.

Defrance, D., Ramstein, G., Charbit, S., Vrac, M., Famien, A. M., Sultan, B., … & Vanderlinden, J. P. (2017). Consequences of rapid ice sheet melting on the Sahelian population vulnerability. Proceedings of the National Academy of Sciences, 114(25), 6533-6538.

Delworth, T. L., Broccoli, A. J., Rosati, A., Stouffer, R. J., Balaji, V., Beesley, J. A., … & Durachta, J. W. (2006). GFDL's CM2 global coupled climate models. Part I: Formulation and simulation characteristics. Journal of Climate, 19(5), 643-674.

Denniston, R. F., Wyrwoll, K. H., Asmerom, Y., Polyak, V. J., Humphreys, W. F., Cugley, J., … & Greaves, E. (2013). North Atlantic forcing of millennial-scale Indo-Australian monsoon dynamics during the Last Glacial period. Quaternary Science Reviews, 72, 159-168.

Dufresne, J. L., Foujols, M. A., Denvil, S., Caubel, A., Marti, O., Aumont, O., … & Bony, S. (2013). Climate change projections using the IPSL-CM5 Earth System Model: from CMIP3 to CMIP5. Climate Dynamics, 40(9-10), 2123-2165.

Dupont, L. M., Schlütz, F., Ewah, C. T., Jennerjahn, T. C., Paul, A., & Behling, H. (2010). Two-step vegetation response to enhanced precipitation in Northeast Brazil during Heinrich event 1. Global Change Biology, 16(6), 1647-1660.

Famien, A. M., Janicot, S., Ochou, A. D., Vrac, M., Defrance, D., Sultan, B., & Noel, T. (2018). A bias-corrected CMIP5 dataset for Africa using the CDF-t method: a contribution to agricultural impact studies. Earth System Dynamics, 9(1), 313-338.

Feddema J (2005) A revised thornthwaite-type global climate classification. Phys Geogr 26(6):442–466

Feng, S., Hu, Q., Huang, W., Ho, C. H., Li, R., & Tang, Z. (2014). Projected climate regime shift under future global warming from multi-model, multi-scenario CMIP5 simulations. Global and Planetary Change, 112, 41-52.

Fraedrich K, Gerstengarbe FW, Werner PC (2001) Climate shifts during the last century. Clim Chang 50(4):405–417

Frieler, K., Lange, S., Piontek, F., Reyer, C. P., Schewe, J., Warszawski, L., ... & Geiger, T. (2017). Assessing the impacts of 1.5 C global warming–simulation protocol of the Inter-Sectoral Impact Model Intercomparison Project (ISIMIP2b). Geoscientific Model Development, 10(12), 4321-4345.

Geiger R (1954) Landolt-Börnstein — Zahlenwerte und Funktionen aus Physik, Chemie, Astronomie, Geophysik und Technik, alte Serie Vol 3. Springer, Berlin

Grimm, E. C., Jacobson, G. L., Watts, W. A., Hansen, B. C., & Maasch, K. A. (1993). A 50,000-year record of climate oscillations from Florida and its temporal correlation with the Heinrich events. Science, 261(5118), 198-200.

Guiot, J., De Beaulieu, J. L., Cheddadi, R., David, F., Ponel, P., & Reille, M. (1993). The climate in Western Europe during the last Glacial/Interglacial cycle derived from pollen and insect remains. Palaeogeography, Palaeoclimatology, Palaeoecology, 103(1-2), 73-93.

Hansen, J., Sato, M., Hearty, P., Ruedy, R., Kelley, M., Masson-Delmotte, V., ... & Velicogna, I. (2016). Ice melt, sea level rise and superstorms: evidence from paleoclimate data, climate modeling, and modern observations that 2 C global warming could be dangerous. Atmospheric Chemistry and Physics, 16(6), 3761-3812.

Kalvová, J., Halenka, T., Bezpalcová, K., & Nemešová, I. (2003). Köppen climate types in observed and simulated climates. Studia Geophysica et Geodaetica, 47(1), 185-202.

Kerschner, H., & Ivy-Ochs, S. (2008). Palaeoclimate from glaciers: Examples from the Eastern Alps during the Alpine Lateglacial and early Holocene. Global and Planetary Change, 60(1-2), 58-71.

Kopp, R. E., DeConto, R. M., Bader, D. A., Hay, C. C., Horton, R. M., Kulp, S., ... & Strauss, B. H. (2017). Evolving understanding of Antarctic ice-sheet physics and ambiguity in probabilistic sea-level projections. Earth's Future, 5(12), 1217-1233.

Köppen, W. (1900). Versuch einer Klassifikation der Klimate, vorzugsweise nach ihren Beziehungen zur Pflanzenwelt. Geographische Zeitschrift, 6(11. H), 593-611.

Köppen W (1923) Die Klimate der Erde: Grundriss der Klima kunde. Walter de Gruyter & Co., Berlin

Köppen W (1931) Grundriss der Klimakunde. Walter de Gruyter & Co., Berlin

Köppen W (1936) Das geographische System der Klimate.In: Köppen W, Geiger R (eds) Handbuch der Klimatologie. Gebrüder Borntraeger, Berlin, p C1–C44

Kottek, M., Grieser, J., Beck, C., Rudolf, B., & Rubel, F. (2006). World map of the Köppen-Geiger climate classification updated. Meteorologische Zeitschrift, 15(3), 259-263.

Lewis, S. C., LeGrande, A. N., Kelley, M., & Schmidt, G. A. (2010). Water vapour source impacts on oxygen isotope variability in tropical precipitation during Heinrich events. Climate of the Past, 6(3), 325-343.

Luan, Y., Braconnot, P., Yu, Y., & Zheng, W. (2015). Tropical Pacific mean state and ENSO changes: sensitivity to freshwater flux and remnant ice sheets at 9.5 ka BP. Climate dynamics, 44(3-4), 661-678.

Mahlstein, I., Daniel, J. S., & Solomon, S. (2013). Pace of shifts in climate regions increases with global temperature. Nature Climate Change, 3(8), 739.

Manabe, S., & Stouffer, R. J. (1980). Sensitivity of a global climate model to an increase of CO_2 concentration in the atmosphere. Journal of Geophysical Research: Oceans, 85(C10), 5529-5554.

Maraun, D. (2016). Bias correcting climate change simulations-a critical review. Current Climate Change Reports, 2(4), 211-220.

Martin, L. C., Blard, P. H., Lavé, J., Condom, T., Prémaillon, M., Jomelli, V., ... & Tibari, B. (2018). Lake Tauca highstand (Heinrich Stadial 1a) driven by a southward shift of the Bolivian High. Science advances, 4(8), eaar2514.

Martinson, D. G. (2012). Antarctic circumpolar current's role in the Antarctic ice system: An overview. Palaeogeography, Palaeoclimatology, Palaeoecology, 335, 71-74.

Marzin, C., Braconnot, P., & Kageyama, M. (2013). Relative impacts of insolation changes, meltwater fluxes and ice sheets on African and Asian monsoons during the Holocene. Climate dynamics, 41(9-10), 2267-2286.

McGuffie, K., Henderson-Sellers, A., Holbrook, N., Kothavala, Z., Balachova, O., & Hoekstra, J. (1999). Assessing simulations of daily temperature and precipitation variability with global climate models for present and enhanced greenhouse climates. International Journal of Climatology: A Journal of the Royal Meteorological Society, 19(1), 1-26.

Meehl, G. A., Boer, G. J., Covey, C., Latif, M., & Stouffer, R. J. (2000). The coupled model intercomparison project (CMIP). Bulletin of the American Meteorological Society, 81(2), 313-318.

Metzger, M.J., Bunce, R.G.H., Jongman, R.H.G., Sayre, R., Trabucco, A. et al., A high-resolution bioclimate map of the world : a unifying framework for global biodiversity research and monitoring. Global Ecology and Biogeography 22, 630–638 (2013).

Michelangeli, P. A., Vrac, M., & Loukos, H. (2009). Probabilistic downscaling approaches: Application to wind cumulative distribution functions. Geophysical Research Letters, 36(11).

Moss, R. H., Edmonds, J. A., Hibbard, K. A., Manning, M. R., Rose, S. K., Van Vuuren, D. P., ... & Meehl, G. A. (2010). The next generation of scenarios for climate change research and assessment. Nature, 463(7282), 747.

Mulitza, S., Prange, M., Stuut, J. B., Zabel, M., von Dobeneck, T., Itambi, A. C., ... & Wefer, G. (2008). Sahel megadroughts triggered by glacial slowdowns of Atlantic meridional overturning. Paleoceanography, 23(4).

Nowlin, W. D., & Klinck, J. M. (1986). The physics of the Antarctic circumpolar current. Reviews of Geophysics, 24(3), 469-491.

Pattyn, F., Ritz, C., Hanna, E., Asay-Davis, X., DeConto, R., Durand, G., ... & Munneke, P. K. (2018). The Greenland and Antarctic ice sheets under 1.5° C global warming. Nature Climate Change, 1.

Peterson, B. J., McClelland, J., Curry, R., Holmes, R. M., Walsh, J. E., & Aagaard, K. (2006). Trajectory shifts in the Arctic and subarctic freshwater cycle. Science, 313(5790), 1061-1066.

Rajaud, A., & de Noblet-Ducoudré, N. (2017). Tropical semi-arid regions expanding over temperate latitudes under climate change. Climatic Change, 144(4), 703-719.

Rignot, E., Velicogna, I., van den Broeke, M. R., Monaghan, A., & Lenaerts, J. T. (2011). Acceleration of the contribution of the Greenland and Antarctic ice sheets to sea level rise. Geophysical Research Letters, 38(5).

Rohli, R.V., Joyner, T.A., Reynolds, S.J. et Ballinger, T.J., Overlap of global Koppen–Geiger climates, biomes, and soil orders. Physical Geography 36, 158–175 (2015).

Rubel, F., & Kottek, M. (2010). Observed and projected climate shifts 1901–2100 depicted by world maps of the Köppen-Geiger climate classification. Meteorologische Zeitschrift, 19(2), 135-141.

Semenov, M. A., & Stratonovitch, P. (2010). Use of multi-model ensembles from global climate models for assessment of climate change impacts. Climate research, 41(1), 1-14.

Sgubin, G., Swingedouw, D., Drijfhout, S., Mary, Y., & Bennabi, A. (2017). Abrupt cooling over the North Atlantic in modern climate models. Nature communications, 8.

Stouffer, R. J., Yin, J., Gregory, J. M., Dixon, K. W., Spelman, M. J., Hurlin, W., ... & Hu, A. (2006). Investigating the causes of the response of the thermohaline circulation to past and future climate changes. Journal of climate, 19(8), 1365-1387.

Stouffer, R. J., Seidov, D., & Haupt, B. J. (2007). Climate response to external sources of freshwater: North Atlantic versus the Southern Ocean. Journal of Climate, 20(3), 436-448.

Swingedouw, D., Fichefet, T., Huybrechts, P., Goosse, H., Driesschaert, E., & Loutre, M. F. (2008). Antarctic ice-sheet melting provides negative feedbacks on future climate warming. Geophysical Research Letters, 35(17).

Swingedouw, D., Mignot, J., Braconnot, P., Mosquet, E., Kageyama, M., & Alkama, R. (2009). Impact of freshwater release in the North Atlantic under different climate conditions in an OAGCM. Journal of Climate, 22(23), 6377-6403.

Swingedouw, D., Rodehacke, C. B., Behrens, E., Menary, M., Olsen, S. M., Gao, Y., Mikolajewicz, U., Mignot, J. and Biastoch, A. (2013). Decadal fingerprints of freshwater discharge around Greenland in a multi-model ensemble, Clim. Dyn., 41(3–4), 695–720.

Swingedouw, D., Rodehacke, C. B., Olsen, S. M., Menary, M., Gao, Y., Mikolajewicz, U., & Mignot, J. (2015). On the reduced sensitivity of the Atlantic overturning to Greenland ice sheet melting in projections: a multi-model assessment. Climate dynamics, 44(11-12), 3261-3279.

Taylor, K. E., Stouffer, R. J., & Meehl, G. A. (2012). An overview of CMIP5 and the experiment design. Bulletin of the American Meteorological Society, 93(4), 485-498.

Trewartha GT, Horn LH (1980) Introduction to climate, 5th edn. McGraw Hill, New York, NY

Vrac, M., Drobinski, P., Merlo, A., Herrmann, M., Lavaysse, C., Li, L., & Somot, S. (2012). Dynamical and statistical downscaling of the French Mediterranean climate: uncertainty assessment. Natural Hazards and Earth System Sciences, 12(9), 2769-2784.

Whitworth III, T. (1988). The Antarctic circumpolar current. Oceanus, 31(2), 53-58.

Supplementary information

SI 1: Koppen classification and formulation given by Kottek *et al* 2006

A	**Equatorial climates**	**Tmin ≥ +18 ∘C**
Af	Equatorial rainforest, fully humid	Pmin ≥ 60 mm
Am	Equatorial monsoon	Pann ≥ 25(100−Pmin)
As	Equatorial savannah with dry summer	Pmin < 60 mm in summer
Aw	Equatorial savannah with dry winter	Pmin < 60 mm in winter

B	**Arid climates**	**Pann < 10 Pth**
BW	Steppe climate	Pann > 5 Pth
BS	Desert climate	Pann ≤ 5 Pth

C	**Warm temperate climates**	**−3 ∘C < Tmin < +18 ∘C**
Cs	Warm temperate climate with dry summer	Psmin < Pwmin, Pwmax > 3 Psmin and Psmin < 40 mm
Cw	Warm temperate climate with dry winter	Pwmin < Psmin and Psmax > 10 Pwmin
Cf	Warm temperate climate, fully humid	neither Cs nor Cw

D	**Snow climates**	**Tmin ≤ −3 ∘C**
Ds	Snow climate with dry summer	Psmin < Pwmin, Pwmax > 3 Psmin and Psmin < 40 mm
Dw	Snow climate with dry winter	Pwmin < Psmin and Psmax > 10 Pwmin
Df	Snow climate, fully humid	neither Ds nor Dw

E	**Polar climates**	**Tmax < +10 ∘C**
ET	Tundra climate	0 ∘C ≤ Tmax < +10 ∘C
EF	Frost climate	Tmax < 0 ∘C

h	Hot steppe / desert	Tann ≥ +18 ∘C
k	Cold steppe /desert	Tann < +18 ∘C

a	Hot summer	Tmax ≥ +22 ∘C
b	Warm summer	not (a) and at least 4 Tmon ≥ +10 ∘C
c	Cool summer and cold winter	not (b) and Tmin > −38 ∘C
d	extremely continental	like (c) but Tmin ≤ −38 ∘C

Tann represents the annual mean temperature. The monthly mean temperatures of the warmest and coldest months are noted by Tmax and Tmin, respectively. The annual precipitation amount corresponds to Pann, and the driest month corresponds to Pmin. Additionally Psmin, Psmax, Pwmin and Pwmax are defined as the lowest and highest monthly precipitation values for the summer and winter half-years on the hemisphere considered. Finally, Pth depends on the annual temperature and the period of the precipitation:

- $2 \times T_{ann}$ if at least 2/3 of the annual precipitation occurs in winte
- $2 \times T_{ann} + 28$ if at least 2/3 of the annual precipitation occurs in summer
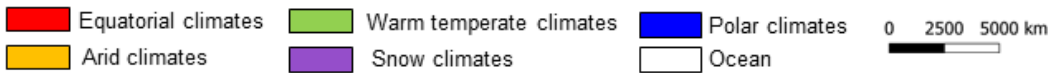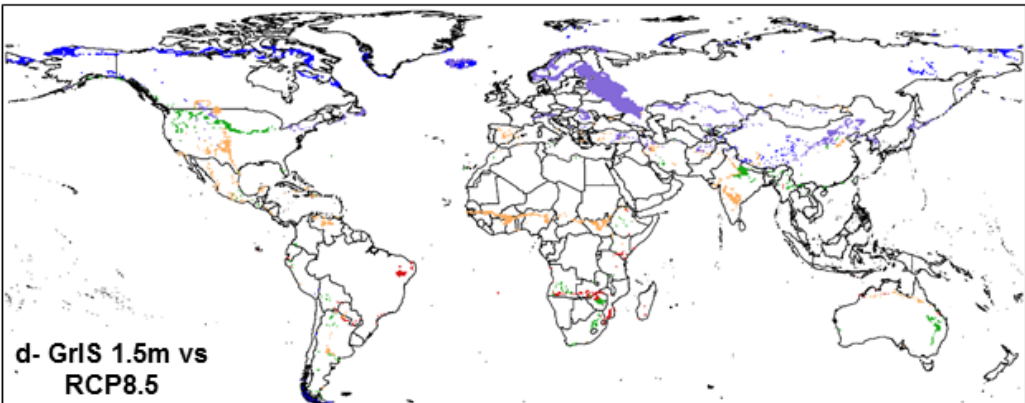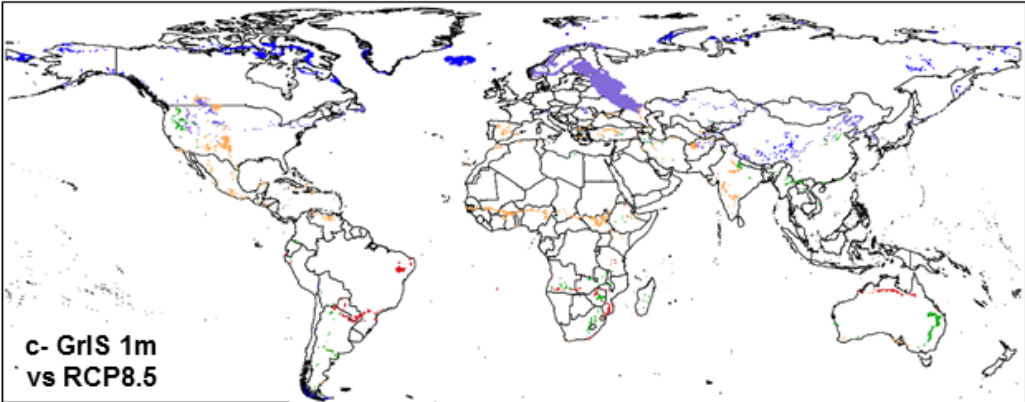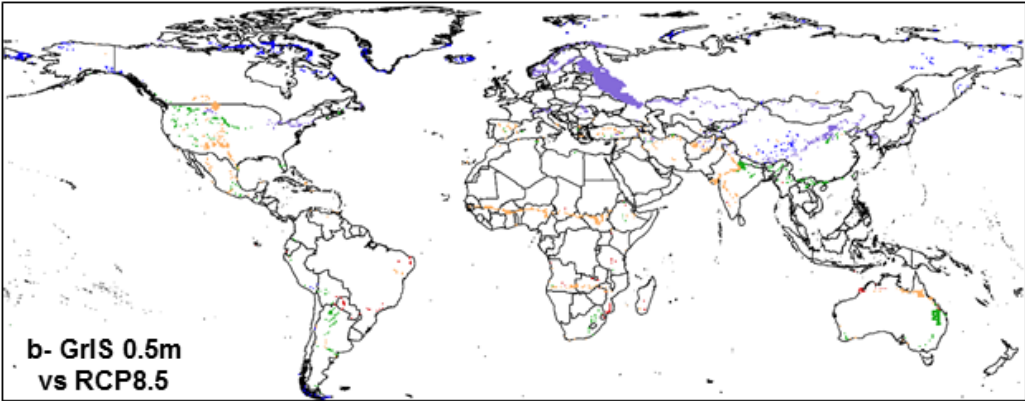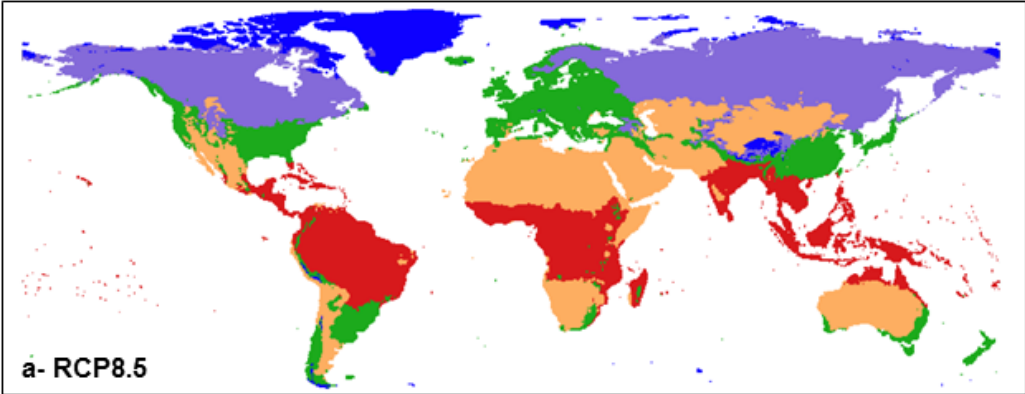- $2 \times T_{ann} + 14$ other cases

SI 2 Difference in temperature between each scenario (2041-2060) and the historical period (1986-2005).
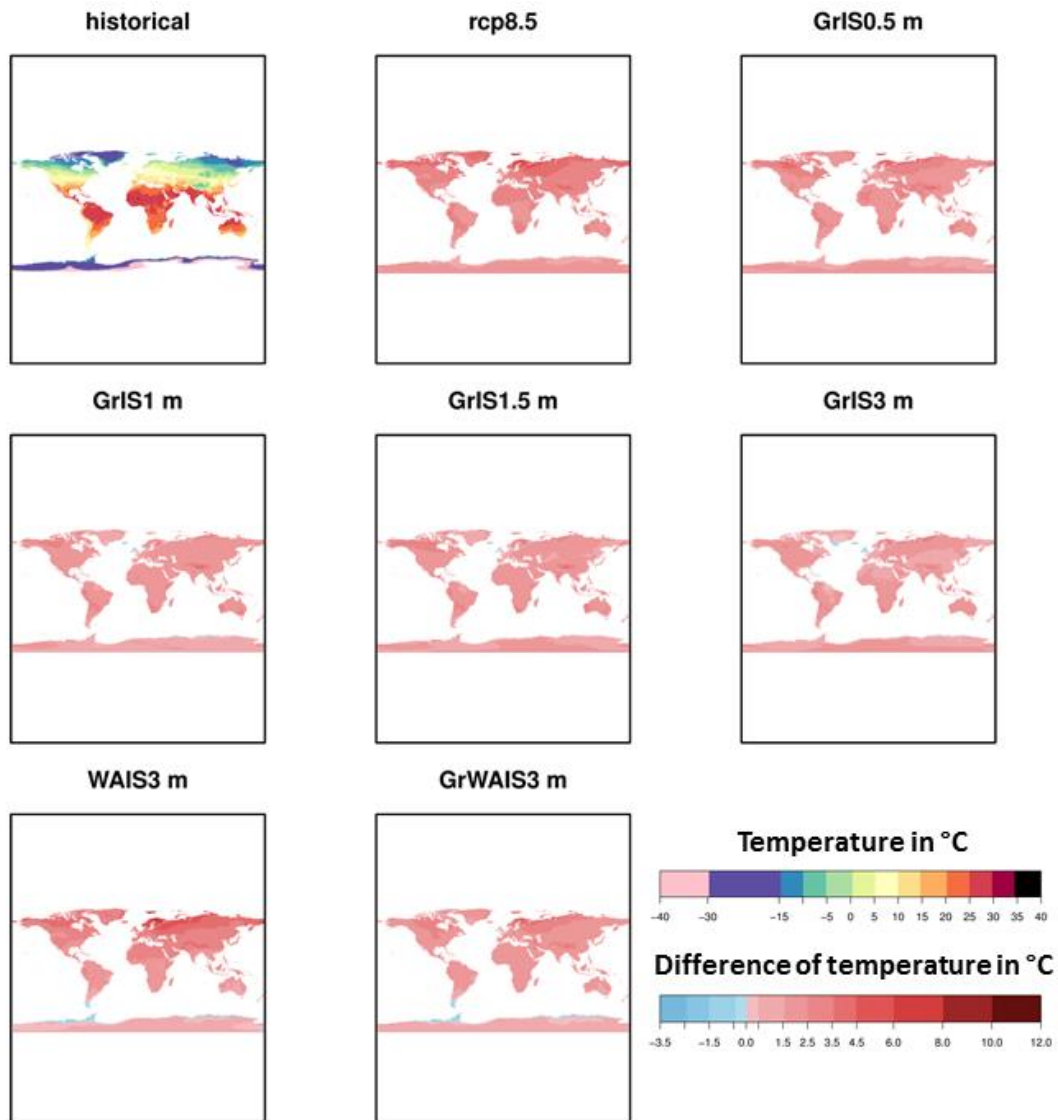
SI 3 Difference in precipitation between each scenario (2041-2060) and the historical period (1986-2005).
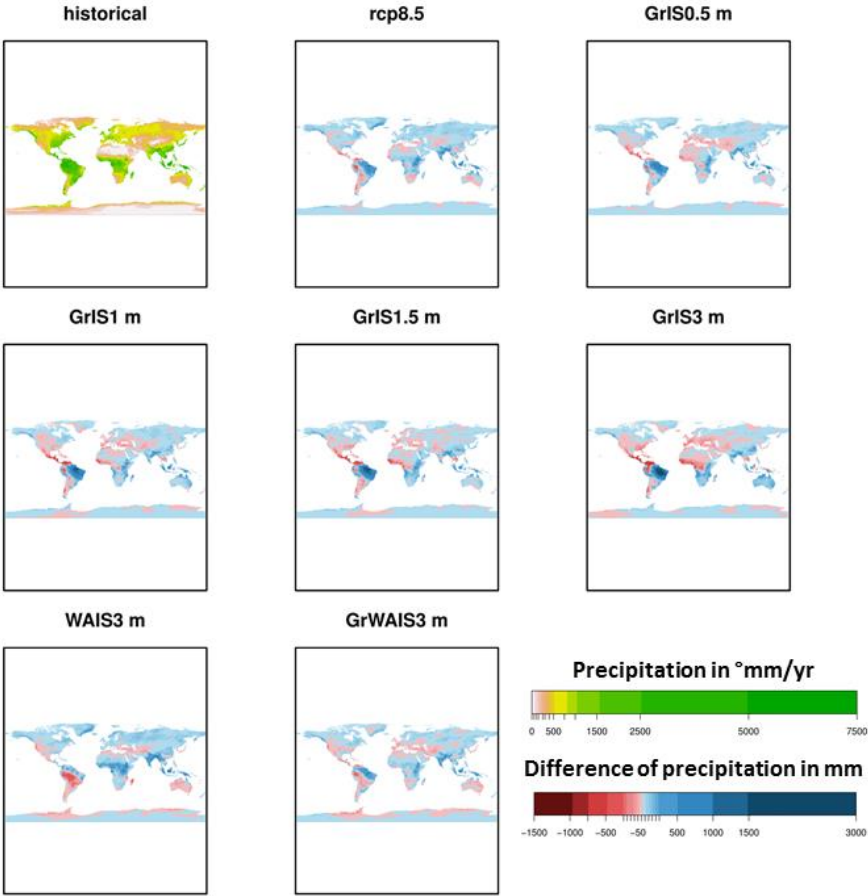
SI4 Group distribution under the RCP8.5 scenario and inter-group changes between various ice melt scenarios and RCP8.5

a- RCP8.5

b- GrIS 0.5m vs RCP8.5

c- GrIS 1m vs RCP8.5

d- GrIS 1.5m vs RCP8.5

■ Equatorial climates	■ Warm temperate climates	■ Polar climates
■ Arid climates	■ Snow climates	□ Ocean

0 2500 5000 km

SI5 Sub-group distribution, based on precipitation, under the RCP8.5 scenario and sub-group changes between various ice melt scenarios and RCP8.5
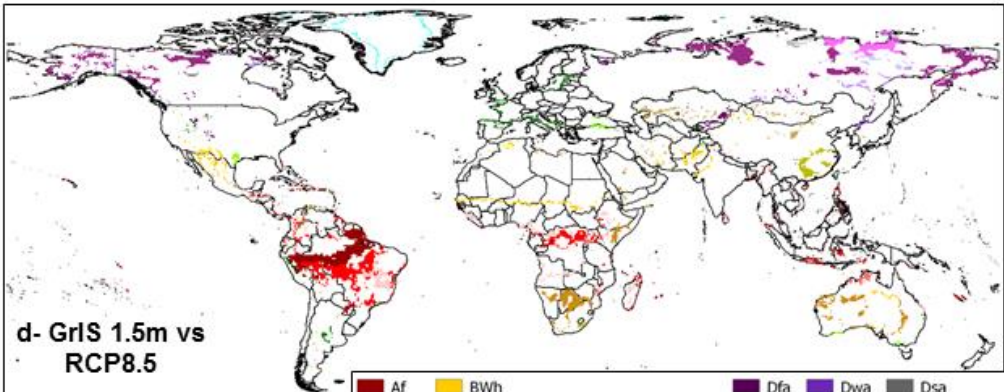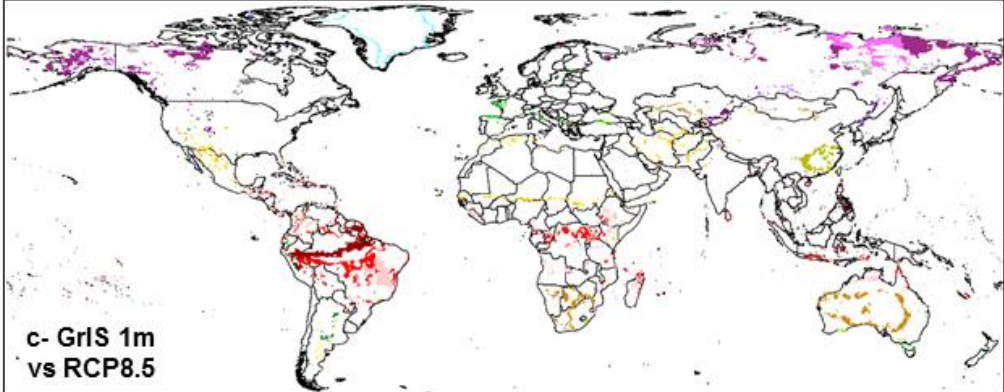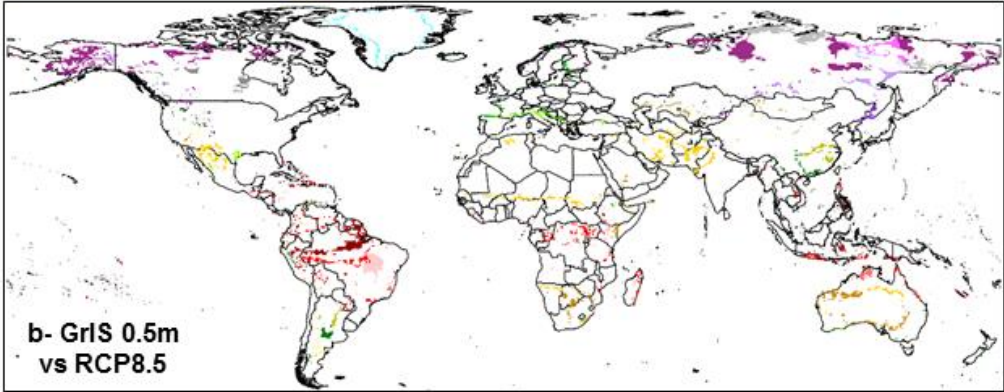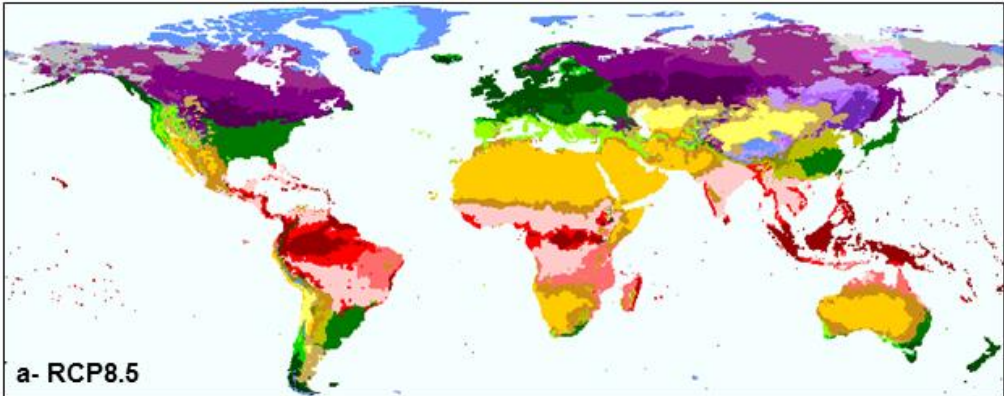
SI6 Sub-group distribution, based on temperature, under the RCP8.5 scenario and sub-group changes between various ice melt scenarios and RCP8.5